Anatomic Evaluation of the Circle of Willis: MR Angiography versus Intraarterial Digital Subtraction Angiography

K. W. Stock, S. Wetzel, E. Kirsch, G. Bongartz, W. Steinbrich, and E. W. Radue

PURPOSE: To evaluate the reliability of source images and maximum intensity projection images of MR angiography in showing the arterial segments of the circle of Willis. **METHODS:** In 62 patients, 526 arterial segments of the circle of Willis were determined to be present, partially present, or absent by blinded observers evaluating MR angiographic source images and maximum intensity projection images. Vessel diameter was measured on source images. These results were then compared with the results from intraarterial digital subtraction angiography. **RESULTS:** MR angiographic maximum intensity projection images had a sensitivity of 87% and a specificity of 88% and MR angiographic source images had a sensitivity of 89% and a specificity of 63% in depicting the presence of a vessel segment. The positive predictive value of an arterial segment with a diameter of at least 1 mm was 99%. **CONCLUSION:** MR angiography is a sensitive technique for detecting the anatomy of the circle of Willis. Maximum intensity projection images are more specific than source images. An arterial segment with a diameter of at least 1 mm on the source image is almost always present and patent.

Index terms: Arteries, magnetic resonance; Efficacy studies; Magnetic resonance angiography

AJNR Am J Neuroradiol 17:1495–1499, September 1996

The size and patency of the arteries of the circle of Willis are variable. Assessment of these characteristics is of interest, because these collaterals influence the clinical outcome of patients with stenoocclusive disease. In patients with an internal carotid artery occlusion or severe stenosis, a small or absent ipsilateral posterior communicating artery is a risk factor for ischemic cerebral watershed infarction (1). We separately compared the findings at arterial digital subtraction angiography (DSA) with findings on angiotomographic source images of a three-dimensional time-of-flight MR angiographic sequence and with the corresponding maximum intensity projection (MIP) images to determine the sensitivities and specificities of MR angiography in depicting the presence of the arteries of the circle of Willis.

Materials and Methods

The findings from 62 patients (40 male, 22 female) who underwent both intraarterial DSA and 3-D time-of-flight MR angiography were reviewed retrospectively to ascertain the presence of the arterial segments of the circle of Willis. The patients were 16 to 78 years old (mean age, 52 years). The indication for DSA was suspicion of stenoocclusive disease (43 patients), tumor (four patients), arteriovenous malformation (five patients), or aneurysm (10 patients). Intraarterial DSA (matrix, 512 × 512) was performed with a 4F or 5F catheter via a femoral artery approach. The catheter was placed into the right and left common carotid arteries, and the basilar artery was imaged by contrast injection into the right and/or left vertebral arteries. In eight patients, there was no DSA study of the basilar artery. The catheter was placed selectively into the internal carotid artery on 29 sides in 18 patients. Contrast material was diluted with saline 0.9% to a concentration of 150 to 250 mg iodine per milliliter and a volume of 7 to 9 mL was injected manually. DSA was performed at two frames per second and included a profile and a half-axial projection of each injected artery. In 25 patients, oblique views of the carotid and/or basilar angiographic sequence were available. DSA revealed an intracranial aneurysm in seven patients, an arteriovenous malforma-

Received December 18, 1995; accepted after revision March 8, 1996.

From the Department of Radiology, University Hospital of Basel, Switzerland.

Address reprint requests to Klaus W. Stock, MD, Department of Radiology, University Hospital of Basel, Petersgraben 4, Ch-4031 Basel, Switzerland.

AJNR 17:1495–1499, Sep 1996 0195-6108/96/1708–1495

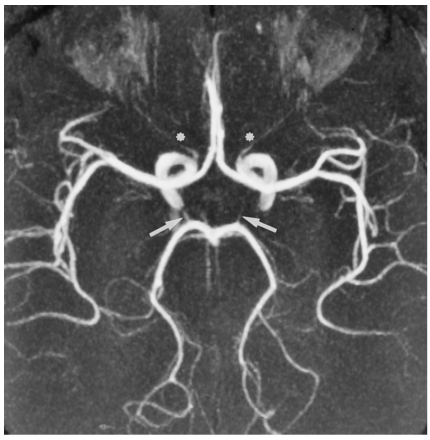

1

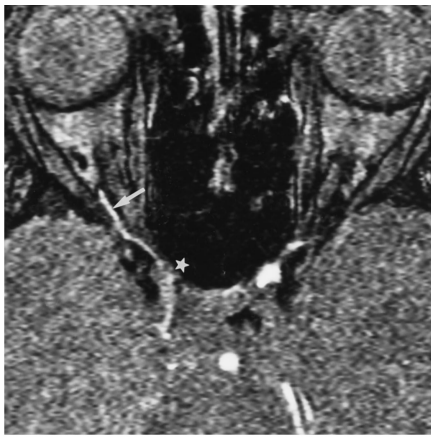

2

Fig 1. MIP image (collapsed view) of the circle of Willis. The anterior communicating artery is not visible. Both posterior communicating arteries can be partially detected *(arrows)*. The proximal segments of the anterior, middle, and posterior cerebral arteries have high signal intensities. The proximal ophthalmic arteries are visible *(asterisks)*.

Fig 2. Source image in a patient with an occluded right internal carotid artery and reversed flow in the right ophthalmic artery. Signal intensity is higher in the right ophthalmic artery *(arrow)* as compared with the low signal intensity in the right internal carotid artery *(star)*. This strongly suggests the presence of an ophthalmic collateral.

tion in three patients, and stenoocclusive disease in 21 patients. One patient had a carotid-cavernous sinus fistula and three patients had an intracranial tumor. DSA showed no intracranial disease in 27 patients.

MR angiography was performed on a 1.5-T unit with a circularly polarized head coil. An axial slab with a thickness of 52 mm and 64 partitions was placed over the entire circle of Willis. A gradient-echo sequence (fast imaging with steady-state precession) with a matrix of 256 × 512 and a field of view of 200 mm was used, which yielded a voxel size of 0.78 × 0.39 × 0.81 mm^3. Additional parameters included 43/8/1 (repetition time/echo time/excitations), bandwidth of 81 Hz per pixel, and acquisition time of 11 minutes 47 seconds. The MR angiographic sequence included a tilted optimized nonsaturating excitation technique with a variable flip angle between 10° at the inlet side and 30° on the outlet side of the slab (nominal flip angle at the slab center was 20°). Additionally, a magnetization transfer saturation pulse was implemented in the MR angiographic sequence to improve background suppression. MIP images of the 64 axial partitions were calculated at 20° increments for a total of 180° for one rotation axis (right to left) (Fig 1).

As much subcutaneous and orbital fat as possible was excluded from the reconstructed volume. The presence of the arterial segments on DSA images was ascertained by one neuroradiologist, a second evaluated the source images (partitions) of the MR angiographic sequence, and a third the MIP images. All three neuroradiologists evaluated one study each. They were blinded to the results of the other imaging techniques; the only common knowledge was the patients' name, birth date, and examination date. The arteries evaluated were the anterior communicating artery and, on both sides, the anterior cerebral artery (A1 segment), the middle cerebral artery (M1 segment), the posterior cerebral artery (P1 segment), and the posterior communicating artery, for a total of nine arterial segments. In the eight patients who did not have DSA of the basilar artery, only the anterior communicating artery and both anterior and middle cerebral arteries (five segments) were evaluated. A total of 526 segments were reviewed. Each segment was marked present, partially present, or not present on one examination form for each imaging technique. Additionally, the size of every visible arterial segment was measured on the MR angiographic source images and categorized into three groups: diameters less than 1 mm, diameters of 1.0 to 2.0 mm, and diameters of 2.1 to 3.0 mm. At the end of the study, the results of the three examination forms were compared. Interobserver variability was investigated from 10 randomly chosen patients (90 arterial segments).

Results

The number of arterial segments determined to be visible, partially visible, or not visible on each of the imaging techniques is summarized in Table 1. Table 2 summarizes the diameters and the positive predictive values of the arterial segments seen and measured on the MR angiographic source images. We calculated sensitivities and specificities for the MR angiographic source images and MIP images, taking DSA as the standard of reference and considering partially visible arterial segments as present. The results are shown in Table 3.

Intraarterial angiography depicted 474 vessel segments as presented and 52 as absent. The MIP images correctly showed 414 of 474 (sensitivity, 87%; positive predictive value, 99%). There were six false-positive findings and 46 true-negative findings, resulting in a specificity of 88% (negative predictive value, 43%). The source images of the MR angiographic sequence correctly depicted 422 arteries (sensitivity, 89%; positive predictive value, 96%). There were 33 true-negative findings and 19 false-positive findings (specificity, 63%; negative predictive value, 39%). Subgroup analysis

TABLE 1: Display of arterial segments

Artery	Intraarterial DSA			MR Angiographic Source Images			MR Angiographic MIP Images		
	Present	Partially Present	Absent	Present	Partially Present	Absent	Present	Partially Present	Absent
Anterior communicating (n = 62)	49	2	11	25	7	30	24	13	25
Posterior communicating (n = 108)	74	5	29	58	8	42	43	9	56
Anterior cerebral (A1 segment) (n = 124)	118	3	3	118	1	5	113	5	6
Middle cerebral (M1 segment) (n = 124)	122	0	2	122	0	2	120	2	2
Posterior cerebral (P1 segment) (n = 108)	100	1	7	99	5	4	89	5	14

TABLE 2: Diameter of arterial segments measured on the MR angiographic source images and their positive predictive value*

Artery	Diameter		
	<1 mm (%)	1.0 to 2.0 mm (%)	2.1 to 3.0 mm (%)
Anterior communicating (n = 32)	27 (81)	5 (100)	0
Posterior communicating (n = 66)	44 (82)	22 (100)	0
Anterior cerebral (A1 segment) (n = 119)	20 (95)	90 (100)	9 (100)
Middle cerebral (M1 segment) (n = 122)	6 (100)	76 (100)	40 (100)
Posterior cerebral (P1 segment) (n = 104)	27 (85)	72 (99)	5 (100)

* Numbers (percentages) represent the positive predictive value.

TABLE 3: Segments of the circle of Willis

Artery	Intraarterial DSA		MR Angiographic Source Images		MR Angiographic MIP Images	
	Present	Absent	True Positive (Sensitivity) (%)	True Negative (Specificity) (%)	True Positive (Sensitivity) (%)	True Negative (Specificity) (%)
Anterior communicating	51	11	26 (51)	6 (55)	34 (67)	8 (73)
Posterior communicating	79	20	59 (75)	21 (72)	50 (63)	27 (93)
Anterior cerebral (A1 segment)	121	3	118 (98)	2 (67)	114 (94)	2 (67)
Middle cerebral (M1 segment)	122	2	122 (100)	2 (100)	122 (100)	2 (100)
Posterior cerebral (P1 segment)	101	7	97 (96)	2 (29)	94 (93)	7 (100)
All segments	474	52	422 (89)	33 (63)	414 (87)	46 (88)

of the anterior and posterior communicating arteries showed a sensitivity of 65% and a specificity of 68% for the source images. On the MIP images a sensitivity of 65% and a specificity of 88% were calculated. The corresponding results for the proximal, middle, and posterior cerebral arteries are as follows: source images, 98% sensitivity and 50% specificity; MIP display, 96% sensitivity and 92% specificity.

DSA revealed eight patients with internal carotid artery obstruction and cross-flow via the anterior communicating artery to the contralateral side to at least the M2 segment. The MIP and source images correctly depicted all A1 and M1 segments as present on the side of the carotid artery obstruction (sensitivity, 100%). Interobserver variability yielded a κ of 0.68 for DSA, 0.67 for the source images, and 0.65 for the MIP display.

At the end of the study we looked, nonblinded, for signs indicating an ophthalmic collateral on the source images. Intraarterial DSA showed seven ophthalmic collaterals in six patients with stenoocclusive disease. Only three could be identified as resulting from a higher signal intensity of the proximal ophthalmic artery as compared with the ipsilateral internal carotid artery, which showed low signal intensity because of slow flow and saturation (Fig 2).

Discussion

In patients with significant flow reduction in either an internal carotid artery or the basilar

artery, collateral arteries can maintain cerebral perfusion in the territory of the affected vessel. Primary collaterals, such as a patent anterior or posterior communicating artery, respond quickly with a higher flow or a reversal of flow direction. Secondary collaterals, such as leptomeningeal anastomoses or an ophthalmic artery collateral, need time to develop until they can contribute a significant blood supply. The configuration of the circle of Willis as primary collaterals at the base of the brain can easily be detected with MR angiography (2–4). MR angiography is noninvasive, and, within 15 minutes, a high-resolution time-of-flight study can be obtained with improved background suppression using a magnetization transfer saturation pulse (5, 6).

We compared the source images of a 3-D time-of-flight MR angiographic sequence and the MIP images with findings at intraarterial DSA, which was the standard of reference. Both the source images and the MIP images showed a good sensitivity (98% and 96%, respectively) in depicting the proximal anterior, middle, and posterior cerebral arteries. Sensitivity was lower for the anterior and posterior communicating arteries (65% and 65%, respectively). The sensitivities are similar to those published by Katz et al (3), who evaluated MIP images of a 3-D phase-contrast MR angiographic sequence. Specificity was acceptable (88%) for the MIP images, but poor (63%) for the angiotomographic source images. Reasons for false-positive findings on the source images might include any of the following: First, the vessel has to be followed through several images and can be confused with another vessel nearby. Second, the posterior communicating artery could be confused with the basal vein or the anterior choroidal artery. Third, a thrombosed artery with high signal due to methemoglobin can be misinterpreted as patent. Fourth, it is possible that a patent vessel is not seen with intraarterial DSA because compression maneuvers and superselective catheterization are not routinely performed. This results in a false-positive finding when the artery is seen with MR angiography. False-negative findings can result from turbulence and saturation effects of slow-flowing blood or long in-plane flow. Therefore, we made a subgroup analysis for the A1 and M1 segments receiving cross-flow blood supply via the anterior communicating artery, resulting in a long in-plane flow. Both MIP and source images showed these segments with, occasionally, attenuated signal intensity. Very small arteries lose their signal intensity because of partial volume effects. A high-resolution MR angiographic sequence is therefore preferred. The MIP display results in loss of visibility of small arteries and of arteries with a low signal intensity, slightly decreasing sensitivity.

Clinically, only collaterals with a diameter of at least 1.0 mm have been shown to be effective in preventing watershed infarction. For this reason we looked at the positive predictive value of the source images for collaterals of this diameter. The vessel diameter was measured on the source images. On the MIP display a reduction of the vessel diameter can occur because of unseen blood near the vessel wall or as a result of the MIP algorithm itself (7). Blood adjacent to the wall has slower velocity and as a consequence low signal intensity due to saturation may be expected. MIP images do not display this low signal intensity, which does not exceed the signal intensity of the background. Underestimation of the vessel diameter on the source images can be attributed to saturation and signal loss of slow-flowing blood, partial volume effects of pixels at the vessel wall, and turbulent flow signal loss. These effects are negated to a certain degree by pulsatile movements of the vessel. With a positive predictive value of 99%, a vessel with a diameter measuring at least 1 mm on the source images has a very high probability of being present and patent, which makes MR angiography clinically useful for seeing the circle of Willis. This is particularly important for patients at risk from significant stenosis or obstruction of an internal carotid artery or basilar arteries. MR angiography could be helpful in evaluating the risk of temporary internal artery occlusion during thromboendarterectomy of the carotid artery or in patients in whom arterial occlusion for treatment of an aneurysm is envisaged (8).

Blood supply to the anterior part of the circle of Willis by reversed flow in the ophthalmic artery is difficult to assess with 3-D time-of-flight MR angiography. Previously, saturation pulses have been used, which we did not do (9). In 43% of ophthalmic arteries with collateral flow, a higher signal intensity in the proximal ophthalmic artery was found as compared with the saturated low signal intensity in the internal carotid artery. This could be a specific sign of an ophthalmic collateral. High signal resulting from

thrombosis can be excluded if vision is normal. A higher signal in the ophthalmic artery can be explained with nonsaturated spins, which do not flow from the saturated internal carotid artery with low signal intensity. Therefore, reversed flow can be assumed.

In conclusion, MR angiography has a high sensitivity and specificity for depicting the anatomy of the circle of Willis. Vessels with a diameter of at least 1 mm on the source image are almost always present and patent. Concerning the anatomy of the circle of Willis, the MIP images were more specific than the source images, although the sensitivities were only slightly different. Higher signal intensity of the ophthalmic artery as compared with the internal carotid artery might be a specific sign of an ophthalmic collateral, but with a sensitivity of 43%, it is not a sensitive finding.

Acknowledgment

We thank B. Behrmann for secretarial work.

References

1. Schomer DF, Marks MP, Steinberg GK, et al. The anatomy of the posterior communicating artery as a risk factor for ischemic cerebral infarction. *N Engl J Med* 1994;330:1565–1570
2. Patrux P, Laissy JP, Jouini S, Kawiecki W, Coty P, Thiébot J. Magnetic resonance angiography (MRA) of the circle of Willis: a prospective comparison with conventional angiography in 54 subjects. *Neuroradiology* 1994;36:193–197
3. Katz DA, Marks MP, Napel SA, Bracci PM, Roberts SL. Circle of Willis: evaluation with spiral CT angiography, MR angiography, and conventional angiography. *Radiology* 1995;195:445–449
4. Edelman RR, Mattle HP, O'Reilly GV, et al. Magnetic resonance imaging of flow dynamics in the circle of Willis. *Stroke* 1990;21: 56–65
5. Dagirmanjian A, Ross JS, Obuchowski N, et al. High resolution, magnetization transfer saturation, variable flip angle, time-of-flight MRA in the detection of intracranial vascular stenoses. *J Comput Assist Tomogr* 1995;19:700–706
6. Edelman RR, Ahn SS, Chien D, et al. Improved time-of-flight MR angiography of the brain with magnetization transfer contrast. *Radiology* 1992;184:395–399
7. Anderson CM, Saloner D, Tsuruda JS, Shapeero LG, Lee RE. Artifacts in maximum-intensity-projection display of MR angiograms. *AJR Am J Roentgenol* 1990;154:623–629
8. Steinberg GK, Drake CG, Peerless SJ. Deliberate basilar or vertebral artery occlusion in the treatment of intracranial aneurysms: immediate results and long-term outcome in 201 patients. *J Neurosurg* 1993;79:161–173
9. Anzola GP, Gasparotti R, Magoni M, Prandini F. Transcranial Doppler sonography and magnetic resonance angiography in the assessment of collateral hemispheric flow in patients with carotid artery disease. *Stroke* 1995;26:214–217